ACS Catalysis

Research Article

pubs.acs.org/acscatalysis

Catalytic Consequences of Particle Size and Chloride Promotion in the Ring-Opening of Cyclopentane on Pt/Al_2O_3

Hui Shi,[†] Oliver Y. Gutiérrez,[†] Hao Yang,[‡] Nigel D. Browning,[§] Gary L. Haller,[†] and Johannes A. Lercher[†,*]

[†]Department of Chemistry and Catalysis Research Center, Technische Universität München, Lichtenbergstraße 4, D-85747 Garching, Germany

[‡]Department of Chemical Engineering and Materials Science, University of California−Davis, One Shields Avenue, Davis, California 95616, United States

[§]Fundamental and Computational Sciences Directorate, Pacific Northwest National Laboratory, Richland, Washington 99352, United States

Supporting Information

ABSTRACT: Ring-opening of cyclopentane on alumina-supported Pt particles was studied as a function of Pt particle size in the presence of different Cl contents. With catalysts prepared from a Cl-free precursor, measured turnover rates increased monotonically with increasing Pt particle size (1−15 nm). On catalysts derived from a Cl-containing precursor, the turnover rates fell into two separate trends with the change of Pt particle size, depending on the extent of Cl removal by increasing thermal treatment temperature. In both cases, catalytic activity increased with increasing particle size in the examined ranges of dispersions (D = 0.7−1.0 and 0−0.6) and for both series of catalysts, the apparent activation energies were higher on large Pt particles than on small ones, with only small differences in the reaction orders for H_2 and cyclopentane on particles of widely varying average sizes. Therefore, the effect of particle size on the turnover rates stems mainly from intrinsic rate constants, rather than from coverage effects. The relative adsorption coefficients of toluene and benzene indicated lower electron densities at the surface Pt atoms in the catalysts prepared from the Cl-containing precursor than in those from the Cl-free precursor. This subtle electron deficiency, which seems not to stem from the local Cl enrichment near Pt, affects both the concentration of chemisorbed hydrogen under reaction conditions and the barrier for C−C bond cleavage. The Cl postintroduced to the catalyst, in contrast, does not induce a similarly positive effect.

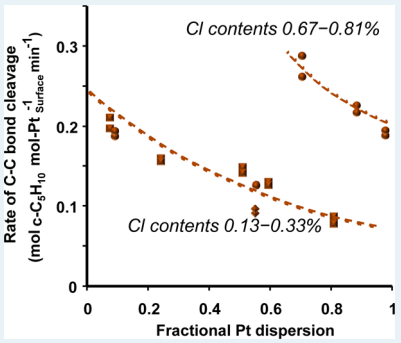

KEYWORDS: *platinum, cyclopentane, ring-opening, structure sensitivity, chloride*

1. INTRODUCTION

Cyclic C_5 molecules are well-established intermediates in the skeletal isomerization of alkanes.[1,2] Compared with its derivative methylcyclopentane (MCP),[1,3−11] cyclopentane (CP) is less frequently studied,[12−15] despite its perceived simplicity for establishing unequivocal structure−activity relations in ring-opening/hydrogenolysis reactions over metal catalysts.

Various particle size dependencies of rates for cyclic C_5 (CP and MCP) ring-opening have been presented over different noble metal catalysts,[12−18] although some were possibly confounded by artifacts such as carbon deposition or adventitious impurities.[19,20] The turnover frequency (TOF) for CP hydrogenolysis at 573 K varied by more than an order of magnitude over Pt/Al_2O_3 catalysts of dispersion 0.05−0.8,[13] as also found with MCP hydrogenolysis on Rh/Al_2O_3 catalysts of dispersion 0.1−1.0.[14] Negligible effects of metal dispersion were, on the other hand, observed for CP hydrogenolysis over Al_2O_3-supported Pd and Ir catalysts.[13,14] For Rh/SiO_2 catalysts, the effects of metal particle size on the TOFs of CP and MCP hydrogenolysis were erratic.[14,15] Increasing TOFs with increasing particle size have been attributed to result from the need of a large ensemble of surface atoms for an active site that is better met on flat surfaces of large particles.[21] These studies were performed at sub- or near-atmospheric H_2 pressures and were, therefore, often accompanied by significant catalyst deactivation.[14] Moreover, the structure sensitivity was explored only at a single set of conditions.

As subtle effects could potentially lead to significant enhancements of catalytic activity, we investigated cyclopentane ring-opening on supported Pt particles with a broad range of dispersions (0.07−0.98) and Cl contents (0.13−0.81 wt %), under conditions that control deactivation by higher H_2 pressures (100−1000 kPa) and H_2-to-hydrocarbon ratios (H_2/CP = 10−150) than in previous reports. At Cl contents lower than 0.33 wt %, measured turnover rates monotonically

Received: September 25, 2012
Revised: December 29, 2012
Published: January 4, 2013

increased with increasing Pt particle size (1−15 nm), along with concomitant decreases in apparent activation barriers. To understand the 2−3 times higher activities, for average particle sizes of 1−2 nm, in catalysts prepared from H_2PtCl_6 compared with those from $Pt(NH_3)_4(NO_3)_2$, we probed the electronic state of Pt by competitive hydrogenation of benzene and toluene. The kinetic data suggest that C−C bond hydrogenolysis is very sensitive to electronic perturbation of surface Pt atoms and that electron-deficient Pt catalyzes the ring-opening of CP more efficiently than relatively neutral Pt atoms. Surprisingly, the presence of Cl postintroduced to the catalyst surface does not induce a similarly positive effect, thus underscoring the importance of choosing chlorinated catalyst precursors for higher C−C bond hydrogenolysis activities.

2. EXPERIMENTAL SECTION

2.1. Catalyst Preparation. $Pt(NH_3)_4(NO_3)_2$ (Aldrich, 97%) was dissolved in doubly distilled water to form an aqueous solution (0.05 M). The catalysts were prepared by incipient wetness impregnation using 1.1 cm^3 of this solution per gram of support (γ/δ-alumina, Evonik Degussa Alu C, 104 $m^2\ g^{-1}$). The impregnated sample was dried at 393 K overnight in flowing dry synthetic air (Westfalen, 20.5 vol % O_2 in N_2) and then treated at 673 K in H_2 flow (101.3 kPa, Westfalen, 99.9999%) for 5 h. The resulting material was divided into five portions treated at various temperatures (573, 673, 773, 873, or 923 K) for 5 h in dry synthetic air flow and then in H_2 flow (101.3 kPa) at 673 K for 5 h. A temperature ramp rate of 1 K min^{-1} was applied for all thermal treatments, and flow rates of 100 $cm^3\ min^{-1}$ (g-sample)$^{-1}$ were applied for all gases. Samples thus prepared are denoted as m%Pt(D)-1/Al_2O_3, where m%, D, and 1 are the actual Pt loading by wt % (AAS), the fractional Pt dispersion (H_2 chemisorption), and a designation of the Cl-free precursor, respectively. A Pt/SiO_2 sample, starting from the same Pt precursor and applying the same treatment protocol as stated above, was named as m%Pt(D)-1/SiO_2.

H_2PtCl_6 (~8 wt % in H_2O, Aldrich) was used to examine the potential effect of Cl on the catalytic performance. The procedure for incipient wetness impregnation and the thermal treatment protocol were the same as for the catalysts prepared from $Pt(NH_3)_4(NO_3)_2$. The resultant samples are denoted as m %Pt(D)-2/Al_2O_3, where m%, D, and 2 are the actual Pt loading by wt % (AAS), the fractional Pt dispersion (H_2 chemisorption), and a designation of the Cl-containing precursor, respectively.

2.2. Catalyst Characterization. *2.2.1. H_2 Chemisorption and N_2 Physisorption.* Hydrogen uptakes were determined volumetrically on a Sorptomatic 1990 instrument. The prereduced catalyst samples were pretreated in 101.3 kPa of stagnant H_2 at 673 K for 2−3 h and then evacuated ($<10^{-1}$ Pa) at the same temperature for 0.5 h before chemisorption measurements at 307 K. An equilibrating time of 2−5 min was used for each pressure increment in a pressure range of 0.5−13.2 kPa. After completing the first isotherm, the sample was evacuated ($<10^{-1}$ Pa, 1 h), and the second isotherm was measured. The amount of chemisorbed hydrogen was determined by extrapolating the linear part (P > 5 kPa) of the difference isotherm (the second isotherm subtracted from the first one) to zero pressure. Dispersions (D), defined as the fraction of Pt atoms exposed at surfaces, were estimated by assuming a $H_{strong}/Pt_{surface}$ stoichiometry of one.[22] Discussion on the consequence of assumed H/Pt_s stoichiometry to the results reported in this study has been placed in the Supporting Information (section S4).

The specific surface areas of the catalyst samples were characterized by N_2 physisorption at 77 K on the Sorptomatic 1990 instrument. Prior to measurements, all samples were outgassed at 523 K for 2 h. The specific BET surface areas were calculated from the adsorption isotherms over a relative pressure range (p/p^0) of 0.03−0.10.

2.2.2. Transmission/Scanning Transmission Electron Microscopy. Samples of the catalysts were ground and ultrasonically dispersed in absolute ethanol for 2 min. Drops of the dispersion were applied on a copper grid-supported carbon film, which upon drying for at least 2 h was introduced into the vacuum system and evacuated before measurement.

Transmission electron micrographs were recorded on a JEM-2010 JEOL transmission electron microscope (TEM) with an accelerating voltage of 120 kV. The STEM/EELS results were obtained using a monochromated, spherical aberration (Cs)-corrected FEI Titan (S)TEM operated at 300 kV. Z-contrast images were collected using a high angle annular dark field (HAADF) detector with a collection angle of 70−190 mrads.

2.2.3. Elemental Analysis. The Pt contents in the catalysts were determined by atomic absorption spectroscopy (AAS) using a UNICAM Solaar M5 spectrometer. Before measurement, typically 50−80 mg of the solid sample was dissolved in 0.5 cm^3 of hydrofluoric acid (10 wt %) at its boiling point (about 383 K).

To analyze the Cl contents, a solid catalyst sample was first fused in a microbomb via vigorous reaction with a mixture of Na_2O_2, K_2CO_3/KNO_3 and ethylene glycol. After cooling the bomb, the contents inside were added with water to a 150 cm^3 beaker and then boiled. The chloride was dissolved into the solution. The titration of Cl in the solution was conducted potentiometrically on a Metrohm 904 Titrando using 0.01 mol L^{-1} $AgNO_3$ as the titrant, Ag^+/S^{2-} as the indicator electrode, and Ag/AgCl as the reference electrode. The results of Pt and Cl contents are shown in Table 1.

2.3. Kinetic Measurements. *2.3.1. Ring-Opening of Cyclopentane.* Ring-opening of cyclopentane (CP) was studied in stainless-steel tubular reactors operated with plug-flow hydrodynamics. Typically, 20 mg of the sieved (180−280 μm) catalyst was diluted with appropriate amounts of acid-washed quartz sand of identical sieve fractions. A K-type thermocouple was attached to the external surface within the isothermal region of the reactor to measure and control the reaction temperature. Less than 1 K difference was detected between temperatures measured on the surface of the reactor or within the catalyst bed. Before reactions, catalysts were pretreated in a pure H_2 (Westfalen AG, 99.999%) flow of 20 $cm^3\ min^{-1}$ from ambient temperature to 623 K, with a ramp rate of 0.167 K s^{-1} and holding for 2 h and then cooled to the reaction temperature (523−563 K). CP was introduced using a flow of He (Westfalen AG, 99.996%) passing through bubblers containing liquid CP (Aldrich, ≥ 99%) in a temperature-controlled water bath. The He flow saturated with CP at the bath temperature was mixed with a flow of H_2 in a cocurrent mode and contacted the catalyst bed to initiate the reaction. Flow rates of gases and total pressures (350−2000 kPa) of the reactor system were modulated by electronic mass flow controllers (Bronkhorst) and back pressure regulators (Bronkhorst). All the kinetic measurements were conducted at differential conditions (<5% conversion) far from equilibrium. The products were analyzed online by a Hewlett-Packard 6890

dx.doi.org/10.1021/cs300636j | ACS Catal. 2013, 3, 328−338

Table 1. BET Surface Area and Pt Dispersions[a] of Supported Pt Catalysts Employed in This Work

	elemental analysis			Pt dispersion (D)	
catalyst	Pt (wt %)	Cl (wt %)	BET surface area ($m^2\ g^{-1}$)	chemisorption	TEM[b]
Pt(0.81)-1/Al_2O_3	0.96	0.20	102	0.81	0.77[c]
Pt(0.59)-1/Al_2O_3	0.98[d]	0.17	98	0.59	0.40
Pt(0.51)-1/Al_2O_3	0.98[d]	n.m.[e]	96	0.51	0.36
Pt(0.24)-1/Al_2O_3	0.96	0.16	97	0.24	0.20
Pt(0.07)-1/Al_2O_3	1.00	0.13	93	0.07	0.07
Pt(0.98)-2/Al_2O_3	1.05	0.81	96	0.98	0.93[c]
Pt(0.88)-2/Al_2O_3	1.03	0.75	94	0.88	0.81[c]
Pt(0.71)-2/Al_2O_3	1.07[d]	0.67	92	0.71	n.m.[e]
Pt(0.55)-2/Al_2O_3	1.04	0.33	95	0.55	0.43
Pt(0.09)-2/Al_2O_3	1.10	0.24	91	0.09	0.08
Pt(0.55)-1/SiO_2	0.41	n.m.[e]	290	0.55	0.44

[a]Measured from H_2 chemisorption uptakes and estimated from electron micrographs. [b]Derived from the average particle diameter ($D = 1.1/d_{av}$ for spherical particle shape). [c]Measured by HAADF-STEM. [d]These are not measured values but were assumed to be the average between the lowest and the highest measured values in the series. [e]Not measured.

Plus GC equipped with a DB Petro column (320 μm × 100 m) and a flame ionization detector. Initial rates and selectivities were reported as values derived by extrapolation of measured steady-state rates and selectivities to zero contact time. Deactivation was minimal (2−5%) during any given reaction time-on-stream.

2.3.2. Competitive Hydrogenation of Benzene and Toluene. The competitive hydrogenation of benzene and toluene was carried out at 308−333 K in a differential, packed-bed tubular reactor at atmospheric total pressure. Benzene (Merck, 99.97%) was distilled from metallic potassium before use. The gas mixture was prepared by passing He through two saturators, containing either benzene or toluene, in two thermostat water baths and mixing with a flow of H_2. H_2 (Westfalen AG, 99.999%) and He (Westfalen AG, 99.996%) were passed through separate purifiers (Supelco). The partial pressures of the hydrocarbons were adjusted by the flow rates of helium and H_2 metered by MFCs. Conversions were kept below 10% in all cases, typically below 5%, and mass and heat transfer limitations were excluded under these conditions. Tests with pure benzene feed were performed on the same setup. Partial hydrogenation products (e.g., cyclohexene/methylcyclohexene) were not detected. Rates reported were measured after 10 min of time-on-stream (TOS) following introduction of reactants.

3. RESULTS AND DISCUSSION

3.1. Particle Size and Dispersion Measurements. Pt contents were similar among the samples and close to the intended value (1.0 wt %; 0.31 Pt-atom nm^{-2}). The catalysts prepared from tetraamine platinum(II) nitrate were found to also contain ≤0.20 wt % Cl (≤0.34 Cl-atom nm^{-2}) because the Al_2O_3 (Degussa Alu C) was prepared from flame hydrolysis of $AlCl_3$ and contained 0.3 wt % Cl initially.[23] The catalysts prepared via impregnating the same Al_2O_3 support with H_2PtCl_6 have a nominal Cl content of 1.1 wt % (Pt loading 1.0 wt %) in the fresh samples. Up to a calcination temperature of 823 K (i.e., Pt(0.98)-2/Al_2O_3, Pt(0.88)-2/Al_2O_3 and Pt(0.71)-2/Al_2O_3), a majority of Cl (0.67−0.81 wt %; 1.1−1.3 Cl-atom nm^{-2}) was retained in the samples. Upon further increasing the calcination temperature to 923 K (i.e., Pt(0.09)-2/Al_2O_3), the majority of Cl was removed, leading to a concentration level (0.24 wt %) comparable to those (0.13−0.20 wt %; 0.22−0.34 Cl-atom nm^{-2}) in the Pt-1/Al_2O_3 catalysts.

Representative transmission electron micrographs are shown in Supporting Information Figure S1, along with corresponding particle size distributions (Supporting Information Figure S2). Representative STEM images for three samples with D = 0.81−0.98 (H_2 chemisorption) are shown in Figure 1. Pt dispersions estimated from TEM/STEM and those obtained from H_2 chemisorption uptakes gave reasonably consistent results (Table 1). Surface-averaged particle diameters ($d_{av} = \Sigma\ n_i d_i^3 / \Sigma\ n_i d_i^2$) were determined from measurement of 140−250 Pt crystallites in TEM images for samples with 0.07−0.55 dispersion and 350−400 Pt particles in HAADF-STEM images for samples with 0.81−0.98 dispersion. TEM/STEM-derived dispersions are typically lower than those from chemisorption uptakes because very small clusters were not detected or not accurately determined. Turnover rates reported hereafter for cyclopentane (CP) ring-opening and arene hydrogenation are based on H_2 chemisorption uptakes because they directly probe the fraction of accessible Pt atoms at particle surfaces.

3.2. Catalytic Activity in the Ring-Opening of Cyclopentane. Under all conditions applied in this work, cyclopentane (CP) was converted almost exclusively (>99%) to *n*-pentane with negligible isomerization or multiple hydrogenolysis. We further note that the high selectivity (>97%) to *n*-pentane was preserved even at higher temperatures (e.g., 593 K), longer contact times, and conversion >40%. Thus, secondary reactions of readsorbed *n*-pentane product did not occur at a significant level on any Pt catalysts, and *n*-pentane did not efficiently compete with the cyclic reactant for the active sites over a wide range of *n*-pentane outlet pressures. Therefore, ring-opening is the only reaction pathway that needs to be evaluated.

Figure 2a shows the mass specific rates of CP ring-opening at 533 K as a function of Pt dispersion. Multiple data points at the same Pt dispersion represent the highest and the lowest measured steady-state rates among at least triplicate kinetic measurements on the same catalyst. The maximum standard deviation was ±5%. The mass-specific activities for Pt-1 and Pt-2/Al_2O_3 catalysts were invariant at D > 0.5 and D > 0.7, respectively, and both decreased thereafter with decreasing Pt dispersion (Figure 2a). For the latter series from the Cl-containing precursor, a significant drop in the specific activity appeared in the dispersion range of 0.6−0.7. Pt/SiO_2 was somewhat less active than the Pt/Al_2O_3 catalysts with similar dispersions (D = 0.5−0.6).

Two separate trend lines, differing by a factor of 2−3, are noted for turnover frequencies (Figure 2b). Along the high-TOF trend lie the three Pt/Al_2O_3 catalysts of high dispersions (D = 0.7−1.0) prepared from H_2PtCl_6 and thermally treated in flowing air at $T \leq 773$ K. The lower line includes all Pt catalysts

dx.doi.org/10.1021/cs300636j | ACS Catal. 2013, 3, 328−338

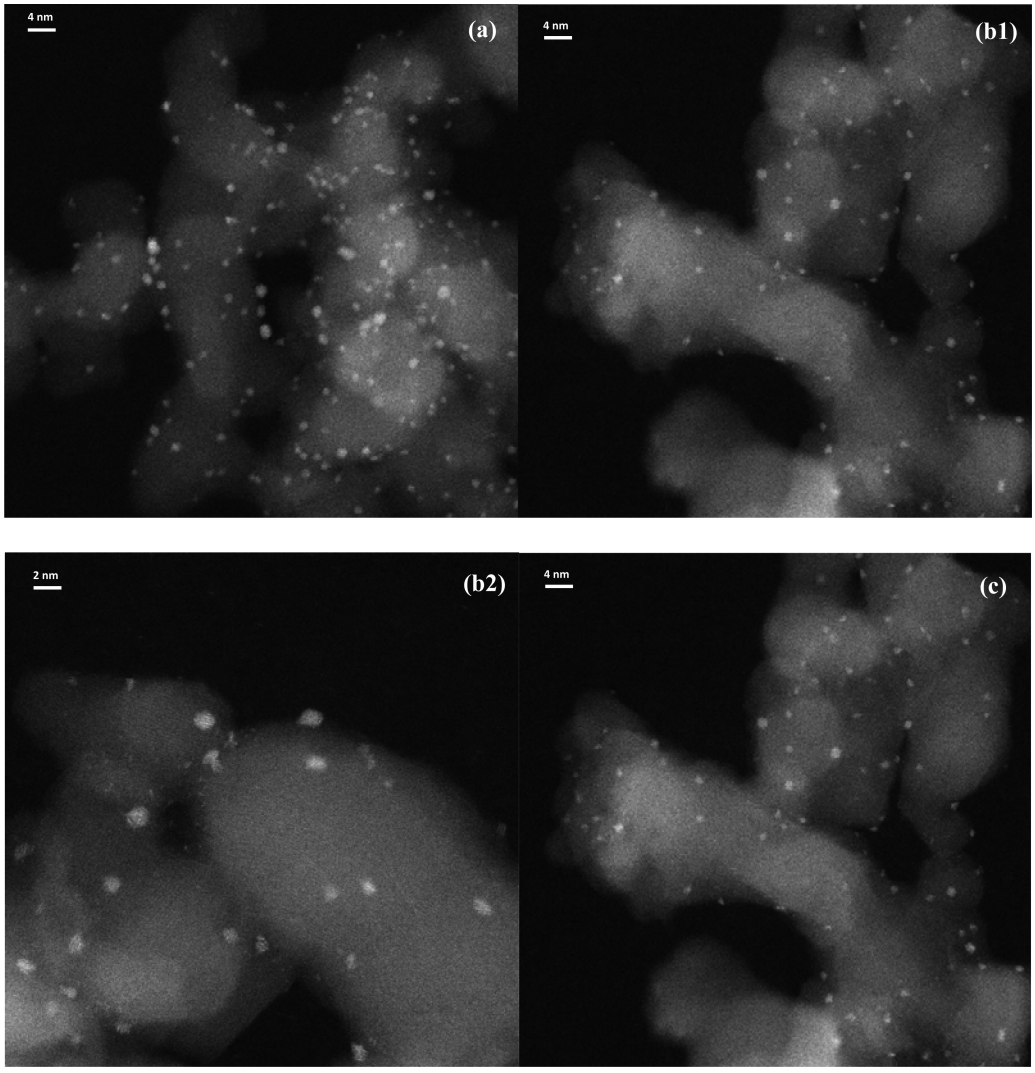

Figure 1. Representative HAADF-STEM images of (a) 0.96%Pt(0.81)-1/Al_2O_3, (b1, b2) 1.05%Pt(0.98)-2/Al_2O_3, and (c) 1.03%Pt(0.88)-2/Al_2O_3.

(Pt/Al_2O_3 and Pt/SiO_2) prepared from the Cl-free precursor as well as two Pt/Al_2O_3 catalysts of lower dispersions (D = 0.09 and 0.55) prepared from H_2PtCl_6 and thermally treated in flowing air at $T \geq 823$ K. Small Pt clusters are less active than larger particles within the first catalyst series (Pt-1/Al_2O_3), but not within the second catalyst series (Pt-2/Al_2O_3). This type of particle size dependence of TOFs, termed "antipathetic structure sensitivity",[21] is qualitatively consistent with previous reports on CP ring-opening (atmospheric pressure) over Pt and Rh catalysts,[13,14] but it contradicts those observed for MCP ring-opening over Pt catalysts.[24]

Over the whole range of H_2 pressures studied, the ring-opening rates decreased with increasing H_2 pressure on all Pt catalysts (Figure 3). The reaction order in H_2 was found to be slightly more negative in the case of Pt-1/Al_2O_3 (Cl-free) than for Pt-2/Al_2O_3; for example, −2.3 to −2.6 vs −1.8 to −2.2 at 500−600 kPa H_2. The difference between the two series was small on catalysts containing mainly large Pt particles (D < 0.30). Moreover, the H_2 order became less negative with decreasing H_2 pressure for both series of catalysts; for example, −1.6 to −1.8 for Pt-1/Al_2O_3 and −1.1 to −1.6 for Pt-2/Al_2O_3 at 100−200 kPa H_2, indicative of maximum rates at even lower H_2 pressures not accessed in this work. The time-on-stream behavior, taking 0.98% Pt(0.59)-1/Al_2O_3 as an example, shows little activity loss upon changing the system pressure, up and then back down (Supporting Information Figure S3).

The reaction order in CP remained 0.60 ± 0.07 over the whole dispersion range for Pt/Al_2O_3 catalysts (Figure 4a). Increasing the H_2 pressure continuously increased the reaction order in CP, indicating depletion of carbonaceous surface intermediates at higher H_2 pressures. Under no circumstances was the surface coverage of CP-derived species negligible, in the light of the smaller-than-unity reaction order (Figure 4b). CP reaction order tended lower (∼0.47) on Pt/SiO_2 than on the Pt/Al_2O_3 catalysts.

In Figure 5, the measured energies of activation for all studied catalysts are compared at the same reactant pressures. For D > 0.7, catalysts prepared from the Cl-free Pt precursor exhibited activation energies higher by ∼40 kJ mol^{-1} than those prepared from the Cl-containing precursor. The difference was smaller at lower dispersions, but still remained as large as 10−20 kJ mol^{-1}. The activation energies were higher at medium to low Pt dispersions, in contrast to the trend in Ir-catalyzed ring-opening of cyclohexane, that is, much lower apparent activation energies at low Ir dispersions.[25] The activation energies measured at varying reactant pressures are compiled in Table 2 for most catalysts. At similar Pt dispersions, apparent activation barriers on Pt-1/Al_2O_3 catalysts were higher than

dx.doi.org/10.1021/cs300636j | ACS Catal. 2013, 3, 328−338

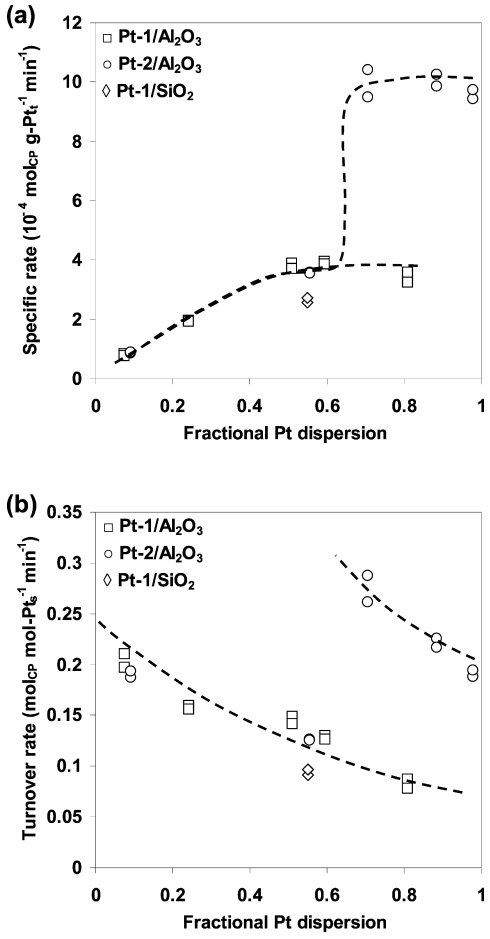

Figure 2. (a) Mass-specific rates and (b) turnover rates of CP ring-opening as a function of Pt dispersion, for (□) Pt-1/Al_2O_3, (○) Pt-2/Al_2O_3, and (◊) 0.41%Pt(0.55)/SiO_2 at 533 K; 8.8 kPa CP and 370 kPa H_2.

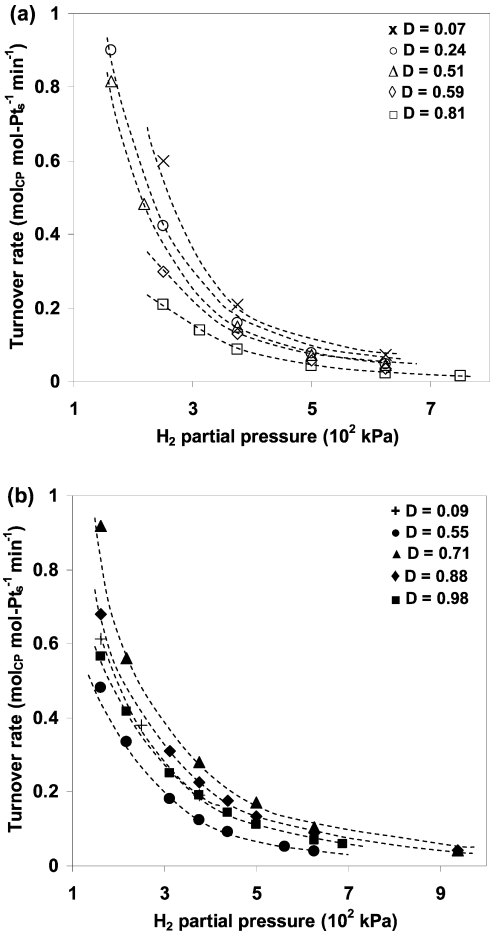

Figure 3. Turnover rates of cyclopentane (CP) ring-opening as a function of H_2 pressure on (a) Pt-1/Al_2O_3 and (b) Pt-2/Al_2O_3 catalysts with varying dispersions at 533 K and 8.8 kPa CP.

those with Pt-2/Al_2O_3 catalysts at all conditions studied. The difference between the two series of catalysts, however, was less pronounced at low H_2 pressures <200 kPa. The activation barriers increased only slightly with increasing H_2 pressure (when >400 kPa) for CP ring-opening over Pt-2/Al_2O_3 catalysts.

Al_2O_3 impregnated with NH_4Cl (1.0 wt % Cl), followed by the same thermal treatments as for the Pt-containing catalysts, did not show any detectable ring-opening activity at temperatures up to 573 K (Supporting Information Table S1), which is below the typical temperatures for acid-catalyzed cracking of alkanes and cycloalkanes.[26] Moreover, hardly any rate enhancement was observed from a mechanical mixture of nonacidic Pt/SiO_2 and the Cl−Al_2O_3, as compared with Pt/SiO_2 (Supporting Information Table S1). Therefore, the Brønsted acidity of the Pt/Al_2O_3 catalysts did not influence the ring-opening activity via a bifunctional route that involves acid-catalyzed C−C bond cleavage in the rate-determining step. The Brønsted or Lewis acidity associated with the hydroxyl groups or residual Cl in the catalyst affected the ring-opening catalysis only indirectly, likely through modifying the electronic or geometric structures of surface Pt atoms that catalyze the reaction. In section 3.4, we develop this discussion in detail.

The above results have shown that the TOF increased with the Pt particle size in the absence of Cl and that the TOFs for CP ring-opening differed by a factor of 2−3 for small Pt clusters obtained from $Pt(NH_3)_4(NO_3)_2$ or H_2PtCl_6 with corresponding differences in the activation energies and the reaction orders in H_2. These changes in the TOF for CP ring-opening are smaller compared with the TOF variations with changing the ionicity of the support in alkane hydrogenolysis.[27,28] In the present work, since the support was unchanged and the particle sizes are similar for small clusters (0.8−1.0 dispersion) in which TOFs varied by more than a factor of 2 between the two series of catalysts (i.e., with and without Cl in the precursor), we consider the electronic state of Pt as the major factor affecting the activity for CP ring-opening. Next, we provide evidence for this hypothesis (section 3.3) and address its microscopic origins on the basis of STEM/EELS studies, theoretical insights in the literature (section 3.4), and a semiqualitative analysis with the Temkin relation (section 3.5).

3.3. Probing the Electronic Density of Small Pt Clusters by Competitive Hydrogenation of Benzene and Toluene. Pt/Al_2O_3 catalysts prepared from $PtCl_6^{2-}$ precursors are often considered to carry a fraction of electron-deficient Pt species, even after reduction, for which evidence was obtained from XPS studies.[23,29,30] For instance, the binding energy of the Pt $4d_{5/2}$ signal was ∼0.4 eV higher with Pt/Al_2O_3 prepared from H_2PtCl_6 than with the catalyst prepared from $Pt(acac)_2$, although both contain similar average Pt particle sizes (1.6−2.0 nm).[30] A comprehensive density functional theory study revealed slightly positive or almost

dx.doi.org/10.1021/cs300636j | ACS Catal. 2013, 3, 328−338

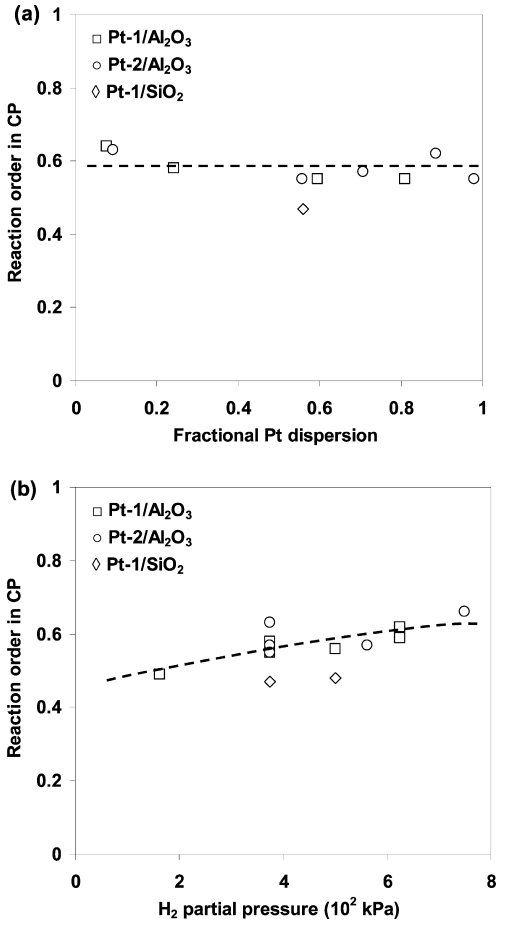

Figure 4. Effects of (a) Pt dispersion (533 K, 6−12 kPa CP and 370 kPa H_2, He balance) and (b) H_2 pressure (533 K, 6−12 kPa CP, He balance) on the reaction order in cyclopentane (CP) for CP ring-opening on Pt catalysts. Multiple symbols at the same H_2 pressure (Figure 4b) were obtained on catalysts of different dispersions. The reaction order in CP was reproducible within ±0.04.

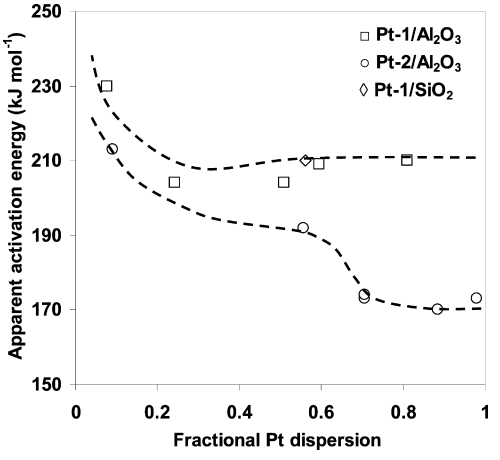

Figure 5. Apparent energies of activation for cyclopentane (CP) ring-opening at 523−563 K, 8.8 kPa CP and 370 kPa H_2 as a function of Pt dispersion. The apparent activation energies were reproducible within ±4 kJ mol^{-1}.

neutral charges associated with small Pt_n clusters ($n \leq 13$) on a chlorinated (110) γ-Al_2O_3 surface.[31]

In this work, we have used a kinetic approach, that is, competitive hydrogenation of benzene and toluene, to assess

Table 2. Apparent Activation Energies in the Ring-Opening of Cyclopentane over Supported Pt Catalysts

	reactant pressure			
catalysts	CP (kPa)	H_2 (10^3 kPa)	$E_{a,app}$[a] (kJ mol^{-1})	H_2 reaction order
Pt(0.81)-1/Al_2O_3	8.8	0.16	182	−1.7
	8.8	0.37	210	−2.0
	12.8	0.27	197	n.m.[b]
Pt(0.59)-1/Al_2O_3	8.8	0.37	209	−2.1
	12.8	0.27	198	n.m.[b]
	11.4	0.63	214	n.m.[b]
Pt(0.24)-1/Al_2O_3	8.8	0.25	198	−1.8
	8.8	0.37	204	−2.1
	12.8	0.27	190	n.m.[b]
Pt(0.07)-1/Al_2O_3	8.8	0.25	207	−1.6
	8.8	0.37	230	−1.9
	12.8	0.27	202	n.m.[b]
Pt(0.98)-2/Al_2O_3	8.8	0.16	152	−1.4
	8.8	0.37	173	−1.6
	12.8	0.27	162	n.m.[b]
	8.8	0.63	177	−1.8
Pt(0.71)-2/Al_2O_3	8.8	0.37	173	−1.9
	12.8	0.27	158	n.m.[b]
	8.8	0.63	177	−2.2
	8.8	0.94	177	n.m.[b]
Pt(0.55)-2/Al_2O_3	8.8	0.16	155	−1.2
	8.8	0.31	192	−1.8
	8.8	0.63	190	−2.1
Pt(0.09)-2/Al_2O_3	8.8	0.19	176	−1.2
	8.8	0.37	213	−1.8
	12.8	0.27	189	n.m.[b]
Pt(0.55)-1/SiO_2	8.8	0.16	180	−1.8
	8.8	0.37	210	−2.4
	12.8	0.27	189	n.m.[b]

[a]Temperature: 523−563 K; uncertainties of ±4 kJ mol^{-1}. [b]Not measured.

the electronic density of surface Pt atoms on small clusters derived from Cl-free or Cl-containing precursors. This methodology correctly reveals the electron density of Pt nanoparticles in the presence of electronic modifiers.[32] Benzene and toluene are adsorbed to the metal surface via π-bonds with electron transfer from the aromatic ring to the unoccupied metal d orbitals. Since toluene is a better electron donor than benzene, as a result of the inductive effect of the methyl group, it adsorbs more strongly than benzene ($K_{T/B} > 1$, where K is the adsorption equilibrium coefficient).[33] Following this idea, Larsen and Haller showed that this $K_{T/B}$ value could also be used to elucidate the electronic states of Pt in zeolite cages.[34] A larger value of $K_{T/B}$ most probably indicates a lower electron density of the surface Pt atoms.[33]

The kinetics of benzene hydrogenation in the absence of toluene were investigated to validate the extraction of relative adsorption coefficients of benzene and toluene on Pt surfaces from benzene hydrogenation rates in benzene/toluene mixtures of different compositions.[33,34] Differences in the turnover rates were small in the hydrogenation of pure benzene, at least over a wide range of Pt dispersions (Figure 6), in accord with the generally observed low sensitivity to particle size for this reaction.[35−42] Large particles were more active, by at most a factor of 2, than small clusters for both series of catalysts (Figure 6), as also found by Flores et al. for Pt/Al_2O_3 catalysts

dx.doi.org/10.1021/cs300636j | ACS Catal. 2013, 3, 328−338

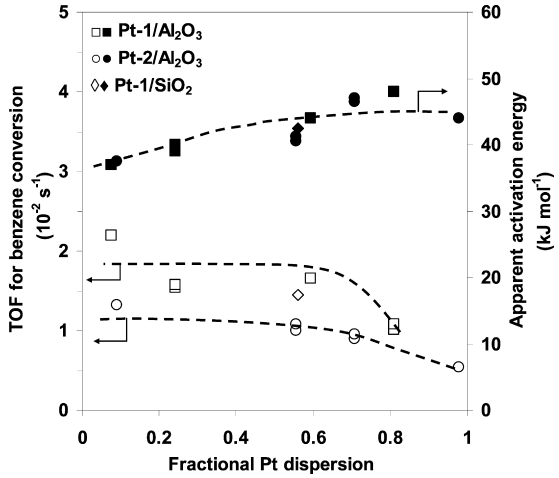

Figure 6. Turnover rates of benzene hydrogenation at 308 K and activation energies as functions of Pt dispersion (2.8 kPa benzene and 62.5 kPa H_2, 36 kPa He balance). The apparent activation energies are reproducible within ±2 kJ mol^{-1}.

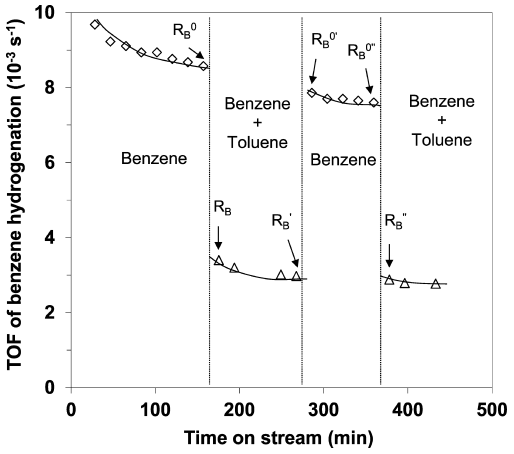

Figure 7. Switch experiment between the feed containing (◊) only benzene and (△) benzene and toluene. Catalyst and reaction conditions: Pt(0.81)-1/Al_2O_3, 308 K, 2.8 kPa benzene, 1.2 kPa toluene, 62.5 kPa H_2, and 34.5 kPa He balance.

reduced at above 673 K.[37] A closer inspection of the rates reveals that the TOFs for benzene hydrogenation are systematically lower on Pt-2/Al_2O_3 catalysts (chlorinated precursor) than on Pt-1/Al_2O_3 catalysts (Figure 6), in contrast to the more-than-doubled TOFs of Pt-2/Al_2O_3 catalysts compared with those of Pt-1/Al_2O_3 series for CP ring-opening (D > 0.6, Figure 2b).

The measured activation energies and orders in two reactants were almost independent of the Pt precursor (Figures 6 and Supporting Information S5). The activation energies increased from 37 to 47 kJ mol^{-1} with decreasing particle size, becoming similar (44 ± 4 kJ mol^{-1}) on sufficiently small (D > 0.6) particles (Figure 6). The reaction order in benzene was slightly positive (~0.07) over all catalysts, whereas the reaction order in H_2 remained in the range of 0.7−0.8 on small (D = 0.6−1.0) Pt clusters and increased to ~1.0 on large (D < 0.3) particles (Supporting Information Figure S5). These values and trends are similar to those in previous reports.[35,36,43]

Previous studies neglected the H-coverage dependence in the Langmuir−Hinshelwood rate expression without justifying this simplification.[32−34] In the present work, we have explored the kinetics of benzene hydrogenation and competitive hydrogenation in greater detail and found that the reaction order in H_2 indeed remained constant on Pt clusters of high dispersions (D = 0.6−1.0), irrespective of the Pt precursor and the absence or presence of toluene (Supporting Information Figure S5). Consequently, it should be valid to derive the relative adsorption coefficients of benzene and toluene ($K_{T/B}$) directly from the hydrogenation rates of benzene in its pure form and in a series of mixtures with toluene (eqs S1−S3, Supporting Information).

Four mixture compositions of benzene and toluene (P_T/P_B = 0.3−1.2) were chosen to evaluate the relative hydrogenation rates (R_B^0/R_B) (Figure 7). We focused on three Pt/Al_2O_3 catalysts containing similarly sized small Pt particles, that is, Pt(0.81)-1/Al_2O_3, Pt(0.88)-2/Al_2O_3, and Pt(0.71)-2/Al_2O_3, which showed turnover rates differing by 2−3 times in the ring-opening of CP (Figure 2b). We chose these catalysts with similar particle sizes (1.1−1.4 nm) because the particle size has a considerable impact on the electronic state of the surface atoms.[44]

Figure 7 shows a typical experiment that switched the feed between 2.8 kPa pure benzene and a mixture with a benzene/toluene ratio of 2.3 (partial pressure). The rates of benzene hydrogenation in the two cases (R_B^0 and R_B) were measured on the same catalyst and at the same reaction temperature. Such switch experiments also made allowance for the deactivation, and in doing so, could reduce the experimental error in the relative ratio of the measured hydrogenation rates (by averaging R_B^0/R_B, $R_B^{0\prime}/R_B{}'$, and $R_B^{0\prime\prime}R_B{}''$ in Figure 7).

Among these three catalysts, the one with the highest dispersion (D = 0.88), derived from H_2PtCl_6, showed the highest $K_{T/B}$ (4.35), slightly higher than Pt(0.71)-2/Al_2O_3 ($K_{T/B}$ = 4.18) which was also prepared from the Cl-containing precursor (Figure 8). Although Pt(0.81)-1/Al_2O_3 had a higher dispersion than Pt(0.71)-2/Al_2O_3, the $K_{T/B}$ value is smaller ($K_{T/B}$ = 3.70) on the former catalyst, suggesting a lower electron density of surface Pt atoms on the latter. This lower electron density does not arise from the particle size because the smaller particle size in Pt(0.81)-1/Al_2O_3 would cause the

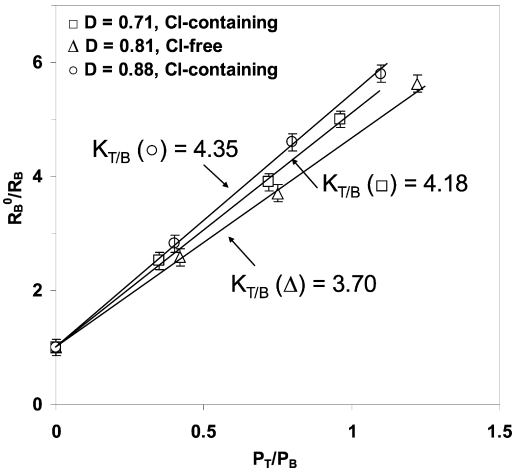

Figure 8. Relative ratios of benzene hydrogenation rates in a pure feed and mixtures of benzene (B) and toluene (T) as a function of the T/B ratio in the gas phase. Reaction conditions: 308 K, 2.8 kPa B, 0−3.4 kPa T, 62.5 kPa H_2, and He balance in a total pressure of 101 kPa. The $K_{T/B}$ values are the slopes of the lines.

dx.doi.org/10.1021/cs300636j | ACS Catal. 2013, 3, 328−338

surface Pt atoms to be more electron-deficient,[27,45] which would have resulted in a larger $K_{T/B}$ value than on Pt(0.71)-2/Al_2O_3.

Although the hydrogenolysis reactions were performed at higher H_2 pressures than those for hydrogenation of arenes, the temperatures were higher for hydrogenolysis than for hydrogenation. Using the predictive contour plot for the H_nPt_{13}/γ-Al_2O_3(100) system in a theoretical work,[47] comparable surface H-loadings were found for the two different sets of conditions. By inference, the effect imposed by adsorbed H atoms on the electronic state of Pt should also be similar in both reactions. Accordingly, we anticipate that the "sensed" electron deficiency should be comparable under hydrogenolysis and hydrogenation conditions used in this study.

The observed differences (4.4 and 4.2 vs 3.7 at 308 K) in the $K_{T/B}$ among Pt(0.88)-2/Al_2O_3, Pt(0.71)-2/Al_2O_3, and Pt(0.81)-1/Al_2O_3 catalysts are much smaller than between Pt clusters encaged in an acidic Y-zeolite and similarly small Pt clusters on a neutral SiO_2 support (14 vs 8 at 298 K).[34] By inference, the electron deficiency of surface Pt atoms is small for Pt-2/Al_2O_3 catalysts. Indeed, CO chemisorption on both series of catalysts failed to disclose this difference in the electron availability in Pt d orbitals (section S1, Supporting Information). Such subtle perturbations to the electronic states of surface Pt atoms may arise from electron-withdrawing chloride species,[46] weakly hydridic adsorbed H atoms,[47] and changes in acidity[48−50] or morphology.[51] We address these possibilities in the next section.

3.4. Origins of the Precursor Effect. It was reported that some of the Cl atoms were still bound to Pt (or the Pt−Al_2O_3 interface) after high-temperature calcination and H_2 reduction.[52] The precursor effect found in this study was, however, unlikely to be the result of nonselective Cl deposition over Pt (i.e., physical blockage), because that would have caused the CP-coverage to change in a more pronounced way than H-coverage due to the larger size of CP compared with H, which was not observed (Figure 4). Direct evidence came from STEM/EELS analysis on the Pt particles (Figure S8, Supporting Information), showing low Cl signal intensities on areas containing only Pt.

Since a direct electron withdrawal from Pt to vicinal Cl atoms was deemed likely to cause the electron deficiency in surface Pt atoms, EEL spectra of the Cl-L edge were recorded by line-scanning the electron probe on Pt-containing areas. A survey of six regions, Supporting Information Figure S9 illustrating a representative example, revealed no enrichment in Cl concentration near Pt particles for Pt-2/Al_2O_3 (H_2PtCl_6 precursor). Postimpregnation of Pt(0.81)-1/Al_2O_3 (Pt-$(NH_3)_4(NO_3)_2$ precursor) with Cl^- ions (see Supporting Information Table S1 for the postsynthetic treatment and reaction data) also increased the activity of the original catalyst to some extent (but not via an acid-catalyzed pathway, section 3.2). The promotional effect (~40%) from these post-introduced Cl, however, was remarkably smaller compared with the difference (2−3 times, Figure 2) between Pt(0.81)-1/Al_2O_3 and Pt-2/Al_2O_3 catalysts with similar dispersions, leading us to conclude that a direct electron transfer from Pt to Cl and higher Cl concentrations in Pt-2/Al_2O_3 catalysts cannot explain the observed 2−3 times higher activities in CP ring-opening.

The observed precursor effect on the electron density of Pt may, in fact, originate from charge transfers from Al surface atoms and migrated H, OH, or Cl species, as suggested by a theoretical study.[31] For instance, Pt clusters can be electron-depleted by the σ Pt−O bond formation induced by migrating H^+ from surface hydroxyl groups.[31] As also shown theoretically, those migrating H^+ can even lead to expansion of the small clusters and increase in the Pt−Al distance in the presence of Cl.[31] This phenomenon may dictate the structural features of 1−2 nm or subnanometric Pt clusters, which thus depend on whether the precursor salt contains Cl. In contrast, a later impregnation of chlorides followed by mild thermal treatments was not as effective. Slight structural differences can, in turn, lead to subtle variations in the electron properties of these small Pt entities yet significantly altering the rates of C−C bond hydrogenolysis. From the available STEM images (Figure 1), however, we have not been successful in conclusively discriminating between particle morphologies in these samples.

Although not fully disregarding the influence of increasing acidity on the electron deficiency of Pt, we believe that this possibility contributes to a minor extent, as the concerned catalysts (Pt-1/Al_2O_3 and Pt-2/Al_2O_3, D = 0.71−0.98) revealed at most a 40% difference in acid concentration (Brønsted and total acidities) from NH_3-TPD experiments (section S5 and Figure S10, Supporting Information). In addition, the less effective promotion of catalytic activity by postintroduced Cl (Supporting Information Table S1) also suggests the increased acidity is not majorly responsible for the 2−3 times higher activities for Pt-2/Al_2O_3 catalysts as compared with Pt-1/Al_2O_3 catalysts.

3.5. Effects of Cl on the Activation Barrier and on the Reactant Coverage. As suggested by the reaction order (Figure 4), the coverage by CP-derived reactive intermediates is changed by <10% by the presence of Cl. Therefore, the difference in rates between Pt-1 and Pt-2 series likely stems from the intrinsic rate constant. Even a small difference of 5−10 kJ mol^{-1} in true activation barrier suffices to account for the difference in the rates or rate constants. The modest difference in the activation barrier is assigned to the subtly altered electronic density of surface Pt atoms.

There is, however, a significant gap in the apparent activation barrier between Pt-1/Al_2O_3 and Pt-2/Al_2O_3 catalysts; the apparent energies of activation are ~40 kJ mol^{-1} higher with the former series than with the latter at high Pt dispersions (Figure 5). The apparent ($E_{a,app}$) and the true ($E_{a,int}$) activation barrier are related by the Temkin equation[53]

$$E_{a,app} = E_{a,int} - \Sigma n_i Q_i \quad (1)$$

where n_i is the order in the reactant i, and Q_i the isosteric heat of adsorption of the reactant i under reaction conditions. It is straightforward from this relation that changes in both the intrinsic activation barrier for C−C bond cleavage (rate-determining) and the enthalpy of the activation of reactants (quasi-equilibrated) can affect the apparent reaction energetics. For catalysts with similar H coverages under reaction conditions (D = 0.55 and 0.71 of Pt-2 series, Table 2), the difference in the measured activation energy reflects mainly that in the intrinsic barrier. Furthermore, it is concluded that the exothermicity term introduced by H_2 adsorption causes the apparent activation barrier to be systematically lower (smaller heat of adsorption and lower reaction orders in H_2), by some 20 kJ mol^{-1}, on the Pt-2/Al_2O_3 catalysts than on Pt-1/Al_2O_3 catalysts with similar dispersions. In contrast, the endothermic term for the activation of CP must be similar, as a result of the similar coverages by CP-derived intermediates indicated by the reaction order in CP. Thus, the presence of Cl facilitates the reaction energetics not only by lowering the intrinsic activation

dx.doi.org/10.1021/cs300636j | ACS Catal. 2013, 3, 328−338

barrier, but also by weakening the H-adsorption and, in turn, decreasing the heat-of-adsorption contribution to the apparent activation barriers.

To support the above analysis, we note that in the ring-opening of CP, H_2 reaction orders (−1.2 to −1.4) observed on Pt-2/Al_2O_3 catalysts were generally less negative than those observed on Pt-1/Al_2O_3 catalysts (−1.6 to −1.8), particularly for small Pt particles (D > 0.7, 100−200 kPa H_2 in Figure 3, Table 2). This suggests that H_2 adsorption on Pt is, indeed, weaker with Pt-2/Al_2O_3 catalyst than with Pt-1/Al_2O_3 catalysts. A weaker H_2 adsorption on Pt-2/Al_2O_3 than on Pt-1/Al_2O_3 catalysts is also consistent with the lower activities of the former in benzene hydrogenation (Figure 6), the rate of which is dictated by a certain H-addition step.

In the hydrogenolysis of neopentane, Koningsberger and co-workers found that the H coverage decreased with increasing acidity of the support.[49,50] These authors reasoned that the surface binding of H atoms was weakened more than C atoms by increasing support acidity because the Pt−H bonding has a greater Pt sp component (Pt 6sp orbitals) than the Pt−C bonding.[49,54,55] In line with this explanation, our experimental results show that the reaction order in CP did not differ appreciably between Pt-1 and Pt-2 series for similar average particle sizes (Figure 4),[56] but the reaction order in H_2 was less negative; H_2 adsorption became less competitive with CP on Pt/Al_2O_3 prepared from hexachloroplatinic acid.

3.6. Origins of the Structure Sensitivity. The turnover rate increased by less than a factor of 3 with Pt particle size increasing from 1 to 15 nm when no Cl-effect was present (Pt-1 series in Figure 2b). Although this was exemplified at a specific set of reaction conditions, it holds also for a wider range of temperatures and reactant pressures (Figures 3−5).

The observed changes of TOFs with Pt dispersion do not correlate with the concentrations of low-coordination atoms (corners and edges), since the number of such sites sharply decreases with increasing particle size (Tables S2 and S3, Supporting Information). Therefore, the higher turnover rates on large particles are related to a higher concentration of low-index planes, in line with a surface-science study performed at near-atmospheric pressures demonstrating that low-index planes are more active for ring-opening/hydrogenolysis catalysis.[57]

Another plausible cause for the increase in catalytic activity with increasing particle size may arise from differences in surface coverage of reactive intermediates, as in the hydrogenolysis of cyclohexane and methylcyclohexane over Ir/Al_2O_3 catalysts;[25,58] however, this effect is rejected because the reaction orders in H_2 and in CP changed little between small and large Pt particles (Table 2 and Figure 4), indicating that the coverages of H_2- and CP-derived intermediates were not much different on small and large Pt particles. In this light, a larger intrinsic rate constant seems more likely to be responsible for the higher TOF on large Pt particles. The rate constant (per surface atom) is higher on large particles, partly because the low-index planes become more abundant on the surface of large particles.[59]

A similar, but more pronounced structure sensitivity for CP ring-opening has been observed over Pt/Al_2O_3 catalysts of varying Pt dispersion.[12,13] This quantitative difference in the scale is due in part to the different reaction conditions. The measured activation energies were larger on low-dispersion than on high-dispersion Pt catalysts by 20−50 kJ mol^{-1} (Figure 5). This necessarily means that reaction rates would show more pronounced differences at higher temperatures between catalysts that feature different activation energies. From the activation energies (170 kJ mol^{-1} at high dispersions, 210 kJ mol^{-1} at low dispersions) and reaction temperatures, the contribution from the rate constant to the magnitude of the structure sensitivity was estimated to be greater by a factor of 2 at 573 K than at 533 K. Therefore, the results in the present work are in good agreement with the change of TOF at 573 K with varying particle size as reported in ref 13. Finally, applying elevated H_2 pressures as in this work controls deactivation to low extents, suggesting that the surface coverage of inactive carbonaceous deposits must be lower than in ref 13. Accordingly, its effect on the structure sensitivity should be minor.[57,60]

Apart from the above-discussed factors, other possible causes have been considered for the dependence of activity on the Pt dispersion, that is, different degrees of reduction and morphological changes for small and large Pt particles. The former can be discarded because the applied reduction temperature (673 K) is sufficient to fully reduce Pt in the presence or absence of Cl,[61] and extended durations (up to 10 h) of H_2-reduction at 673 K for high-dispersion Pt/Al_2O_3 catalysts did not change the catalytic activities to an appreciable extent (not shown). Morphological changes of Pt particles may be responsible for the drastic TOF variations between Pt-2/Al_2O_3 catalysts calcined at 773 and 873 K (D = 0.71 and 0.55, respectively); however, the morphology change expected with increasing treatment temperatures, that is, from 3D to flat raftlike structures, would result in a smaller number of nearest neighbors for Pt and, concomitantly, a decreased electron density.[51]

4. CONCLUSIONS

Ring-opening of cyclopentane (CP) has been studied over supported Pt catalysts under varying H_2 pressures. For the catalysts prepared from the Cl-free precursor, turnover rates increased monotonically with increasing average Pt particle size. For those prepared from the Cl-containing precursor, turnover rates exhibited two branches of increasing TOFs with increasing particle size. TOFs of these catalysts with D = 0.09−0.55, which retained no more than 0.33 wt % Cl, lay on the same trend line as for the Pt-1/Al_2O_3 series. However, the catalysts with D = 0.71−0.98, which contained more than 0.67 wt % Cl, lay on a different trend line, exhibiting a promotional effect (2−3 times) of using the Cl-containing Pt precursor. In contrast, activity enhancement was less marked (40%) when a similar concentration of Cl was introduced to the catalyst by postimpregnation.

The limited changes in the reaction orders in CP and H_2 on Pt particles of different sizes in the absence of Cl-effect lead us to conclude that the higher turnover rates on large Pt particles are mainly due to the higher intrinsic rate constants per surface atom, which depend on the fraction of catalytically more active surface low-index planes. We conclude that the unique enhancement effect of using the Cl-containing precursor on the TOF for ring-opening of CP is caused by the decreased electron density of Pt, which consequently lowers the activation barrier and also the concentration of H adatoms on the surface Pt atoms.

The ratio of adsorption coefficients of toluene and benzene on Pt has been utilized as a quantitative measure of these relative electronic densities of surface Pt species in catalysts prepared from the Cl-free and Cl-containing precursors.

dx.doi.org/10.1021/cs300636j | ACS Catal. 2013, 3, 328−338

STEM/EELS analysis indicated no Cl enrichment near the Pt atoms in the latter catalysts.

■ ASSOCIATED CONTENT

Supporting Information

Transmission and scanning transmission electron micrographs, EELS spectra, and Pt particle size distributions for representative Pt/Al_2O_3 samples, procedures and results of infrared CO adsorption experiments, NH_3-TPD experiments, effect of Pt dispersion on the reaction orders with respect to H_2 and benzene in benzene hydrogenation, derivation of rate equation for competitive hydrogenation of benzene and toluene, estimated population of different types of surface atoms in idealized geometric models. This information is available free of charge via the Internet at http://pubs.acs.org/.

■ AUTHOR INFORMATION

Corresponding Author

*Fax: +49 89 28913544. E-mail: johannes.lercher@ch.tum.de.

Notes

The authors declare no competing financial interest.

■ ACKNOWLEDGMENTS

Hui Shi thanks the Elitenetzwerk Bayern NanoCat for a Ph.D. grant and financial support. The authors are indebted to Dipl.-Ing. Xaver Hecht for technical support and for conducting N_2 physisorption and H_2 chemisorption measurements, to Dipl.-Ing. Martin Neukamm for conducting AAS measurements, and to Ms. Ulrike Ammari for help with the Cl analysis. The authors also are thankful for the support from EMSL, a national scientific user facility located at Pacific Northwest National Laboratory, which is operated by Battelle for the U.S. Department of Energy under Contract No. DE-AC05-76RL01830. We are also grateful to Dr. George D. Meitzner (Edge Analytical, Inc.) for his critical reading of the manuscript.

■ REFERENCES

(1) Gault, F. G. *Adv. Catal.* **1981**, *30*, 1−95.
(2) Barron, Y.; Maire, G.; Cornet, J. M.; Muller, J. M.; Gault, F. G. *J. Catal.* **1963**, *2*, 152−155.
(3) Hayek, K.; Kramer, R.; Paál, Z. *App. Catal., A* **1997**, *162*, 1−15.
(4) Kramer, R.; Zuegg, H. *J. Catal.* **1983**, *80*, 446−456.
(5) Zaera, F.; Godbey, D.; Somorjai, G. A. *J. Catal.* **1986**, *101*, 73−80.
(6) Samoila, P.; Boutzeloit, M.; Especel, C.; Epron, F.; Marécot, P. *J. Catal.* **2010**, *276*, 237−248.
(7) Samoila, P.; Boutzeloit, M.; Salem, I.; Uzio, D.; Mabilon, G.; Epron, F.; Marecot, P.; Especel, C. *Appl. Catal., A* **2012**, *415*, 80−88.
(8) Djeddi, A.; Fechete, I.; Garin, F. *Appl. Catal., A* **2012**, *413*, 340−349.
(9) Zhao, Z. J.; Moskaleva, L. V.; Rösch, N. *J. Catal.* **2012**, *285*, 124−133.
(10) Paál, Z.; Győrffy, N.; Wootsch, A.; Tóth, L.; Bakos, I.; Szabó, S.; Wild, U.; Schlögl, R. *J. Catal.* **2007**, *250*, 254−263.
(11) Alvarez, W. E.; Resasco, D. E. *J. Catal.* **1996**, *164*, 467−476.
(12) Barbier, J.; Morales, A.; Marécot, P.; Maurel, R. *Bull. Soc. Chim. Belg.* **1979**, *88*, 569−576.
(13) Barbier, J.; Marecot, P. *Nouv. J. Chim.* **1981**, *5*, 393−396.
(14) Del Angel, G. A.; Coq, B.; Ferrat, G.; Figuéras, F. *Surf. Sci.* **1985**, *156*, 943−951.
(15) Fuentes, S.; Figuéras, F. *J. Catal.* **1980**, *61*, 443−453.
(16) Coq, B.; Dutartre, R.; Figuéras, F.; Tazi, T. *J. Catal.* **1990**, *122*, 438−447.
(17) Barbier, J.; Marécot, P.; Morales, A.; Maurel, R. *Bull. Soc. Chim. Fr.* **1978**, 309−310.
(18) Coq, B.; Bittar, A.; Figuéras, F. *Appl. Catal.* **1990**, *59*, 103−121.
(19) Fuentes, S.; Figuéras, F. *J. Chem. Soc. Faraday Trans.* **1978**, *74*, 174−181.
(20) Wild, U.; Teschner, D.; Schlögl, R.; Paál, Z. *Catal. Lett.* **2000**, *67*, 93−98.
(21) Che, M.; Bennett, C. O. *Adv. Catal.* **1989**, *36*, 55−172.
(22) Vannice, M. A.; Benson, J. E.; Boudart, M. *J. Catal.* **1970**, *16*, 348−356.
(23) Jackson, S. D.; Willis, J.; McLellan, G. D.; Webb, G.; Keegan, M. B. T.; Moyes, R. B.; Simpson, S.; Wells, P. B.; Whyman, R. *J. Catal.* **1993**, *139*, 191−206.
(24) Anderson, J. R.; Shimoyama, Y. In *Proceedings of the 5th International Congress on Catalysis*, 4th ed.; Hightower, J. W., Ed.; North-Holland: Amsterdam, 1973; Vol. *1*, p 695.
(25) Shi, H.; Li, X. B.; Haller, G. L.; Gutiérrez, O. Y.; Lercher, J. A. *J. Catal.* **2012**, *295*, 133−145.
(26) Du, H.; Fairbridge, C.; Yang, H.; Ring, Z. *Appl. Catal., A* **2005**, *294*, 1−21.
(27) Miller, J. T.; Meyers, B. M.; Modica, F. S.; Vaarkamp, M.; Koningsberger, D. C. *J. Catal.* **1993**, *143*, 395−408.
(28) Boudart, M.; Dalla Betta, R. A. In *Proceedings of the 5th International Congress on Catalysis*, 4th ed.; Hightower, J. W., Ed.; North-Holland: Amsterdam, 1973; Vol. *2*, p 1329.
(29) Reyes, P.; Oportus, M.; Pecchi, G.; Fréty, R.; Moraweck, B. *Catal. Lett.* **1996**, *37*, 193−197.
(30) Karhu, H.; Kalantar, A.; Väyrynen, I. J.; Salmi, T.; Murzin, D. Y. *Appl. Catal., A* **2003**, *247*, 283−294.
(31) Mager-Maury, C.; Chizallet, C.; Sautet, P.; Raybaud, P. *ACS Catal.* **2012**, *2*, 1346−1357.
(32) Guo, Z.; Chen, Y. T.; Li, L. S.; Wang, X. M.; Haller, G. L.; Yang, Y. H. *J. Catal.* **2010**, *276*, 314−326.
(33) Phuong, T. T.; Massardier, J.; Gallezot, P. *J. Catal.* **1986**, *102*, 456−459.
(34) Larsen, G.; Haller, G. L. *Catal. Lett.* **1989**, *3*, 103−110.
(35) Lin, S. D.; Vannice, M. A. *J. Catal.* **1993**, *143*, 539−553.
(36) Lin, S. D.; Vannice, M. A. *J. Catal.* **1993**, *143*, 554−562.
(37) Flores, A. F.; Burwell, R. L.; Butt, J. B. *J. Chem. Soc. Faraday Trans.* **1992**, *88*, 1191−1196.
(38) Basset, J. M.; Dalmai-Imelik, G.; Primet, M.; Mutin, R. *J. Catal.* **1975**, *37*, 22−36.
(39) Bond, G. C. *Surf. Sci.* **1985**, *156*, 966−981.
(40) Maurel, R.; Leclercq, G.; Barbier, J. *J. Catal.* **1975**, *37*, 324−331.
(41) Cunha, D. S.; Cruz, G. M. *Appl. Catal., A* **2002**, *236*, 55−66.
(42) Henry, C. R.; Chapon, C.; Giorgio, S.; Goyhenex, C. In *Chemisorption and Reactivity on Supported Clusters and Thin Films: Towards an Understanding of Microscopic Processes in Catalysis*; Lambert, R. M., Pacchioni, G., Eds.; Kluwer: Dordrecht, 1997; p 117.
(43) Pushkarev, V. V.; An, K.; Alayoglu, S.; Beaumont, S. K.; Somorjai, G. A. *J. Catal.* **2012**, *292*, 64−72.
(44) Guczi, L.; Pászti, Z.; Pető, G. In *Metal Nanoclusters in Catalysis and Materials Science: The Issue of Size Control*; Corain, B., Schmid, G., Toshima, N., Eds.; Elsevier: Amsterdam, 2008; p 77.
(45) Vaarkamp, M.; Miller, J. T.; Modica, F. S.; Lane, G. S.; Koningsberger, D. C.; Uematsu, T.; Haller, G. L.; Haensel, V.; Klier, K.; Renouprez, A.; Joyner, R. W.; Prins, R. *Stud. Surf. Sci. Catal.* **1993**, *75*, 809−820.
(46) Fanson, P. T.; Delgass, W. N.; Lauterbach, J. *J. Catal.* **2001**, *204*, 35−52.
(47) Mager-Maury, C.; Bonnard, G.; Chizallet, C.; Sautet, P.; Raybaud, P. *ChemCatChem* **2011**, *3*, 200−207.
(48) Williams, M. F.; Fonfé, B.; Woltz, C.; Jentys, A.; van Veen, J. A. R.; Lercher, J. A. *J. Catal.* **2007**, *251*, 497−506.
(49) Koningsberger, D. C.; Oudenhuijzen, M. K.; De Graaf, J.; Van Bokhoven, J. A.; Ramaker, D. E. *J. Catal.* **2003**, *216*, 178−191.
(50) Mojet, B. L.; Miller, J. T.; Ramaker, D. E.; Koningsberger, D. C. *J. Catal.* **1999**, *186*, 373−386.
(51) Vaarkamp, M.; Miller, J. T.; Modica, F. S.; Koningsberger, D. C. *J. Catal.* **1996**, *163*, 294−305.
(52) Zhou, Y.; Wood, M. C.; Winograd, N. *J. Catal.* **1994**, *146*, 82−86.

(53) Temkin, M. *Acta Physicochim. URSS* **1935**, *3*, 312−316.
(54) Oudenhuijzen, M. K.; Van Bokhoven, J. A.; Miller, J. T.; Ramaker, D. E.; Koningsberger, D. C. *J. Am. Chem. Soc.* **2005**, *127*, 1530−1540.
(55) Kua, J.; Goddard, W. A. *J. Phys. Chem. B* **1998**, *102*, 9481−9491.
(56) As the H coverage decreases, the coverage by CP-derived intermediates has to increase, leading to smaller reaction orders in CP. However, this change in the CP reaction order is more difficult to discern compared with the reaction order in H_2, as analyzed in the Supporting Information.
(57) Herz, R. K.; Gillespie, W. D.; Peterson, E. E.; Somorjai, G. A. *J. Catal.* **1981**, *67*, 371−386.
(58) Shi, H.; Gutiérrez, O. Y.; Haller, G. L.; Mei, D.; Rousseau, R.; Lercher, J. A. *J. Catal.* **2013**, *297*, 70−78.
(59) Van Hardeveld, R.; Hartog, F. *Surf. Sci.* **1969**, *15*, 189−230.
(60) Gillespie, W. D.; Herz, R. K.; Peterson, E. E.; Somorjai, G. A. *J. Catal.* **1981**, *70*, 147−159.
(61) Lieske, H.; Lietz, G.; Spindler, H.; Völter, J. *J. Catal.* **1983**, *81*, 8−16.